Intelligent Built-In Torque Sensor for Harmonic Drive Systems

Hamid D. Taghirad and P. R. Bélanger

***Abstract*— The unique performance features of harmonic drives, such as highs gear ratios and high torque capacities in a compact geometry, justify their widespread industrial application especially in many electrically actuated robot manipulators. In many robotic control strategies it is assumed that the actuator is acting as a torque source, and in order to implement such algorithms it is necessary to accurately measure the transmitted torque by the harmonic drive. In this paper a built-in torque sensor for harmonic drive systems is developed and examined in detail, in which strain-gauges are directly mounted on the harmonic drive flexspline. To minimize sensing inaccuracy, four Rosette strain gauges are used employing an accurate positioning method. To cancel the torque ripples, the oscillation observed on the measured torque and caused mainly by gear teeth meshing, Kalman filter estimation is used. A simple fourth order harmonic oscillator proved to accurately model the torque ripples. Moreover, the error model is extended to incorporate any misalignment torque. By on line implementation of the Kalman filter, it has been shown that this method is a fast and accurate way to filter torque ripples and misalignment torque. Hence, the intelligent built-in torque sensor is a viable and economical way to measure the harmonic drive transmitted torque and to employ that for torque feedback strategies.**

***Index Terms*— Built-in torque sensor, harmonic drive, intelligent sensor, Kalman filter, misalignment torque, positioning error, rosette strain gauge, torque ripples.**

I. Introduction

DEVELOPED in 1955 primarily for aerospace applications, harmonic drives are high-ratio and compact torque transmission systems. Every harmonic drive consists of the three components illustrated in Fig. 1. The wave generator is a ball bearing assembly with a rigid, elliptical inner race and a flexible outer race. The flexspline is a thin-walled, flexible cup adorned with small, external gear teeth around its rim. The circular spline is a rigid ring with internal teeth machined along a slightly larger pitch diameter than those of the flexspline. When assembled, the wave generator is nested inside the flexspline, causing the flexible circumference to adopt the elliptical profile of the wave generator, and the external teeth of the flexspline to mesh with the internal teeth on the circular spline along the major axis of the wave generator ellipse.

If properly assembled, all three components of the transmission can rotate at different but coupled velocities on the same axis. To use the harmonic drive for speed reduction, the wave generator is mounted on the electric motor shaft, and the output is conveyed either through the circular spline while the flexspline is fixed or through the flexspline while the circular spline is fixed. In the latter case, by rotation of the wave generator the zone of gear-tooth engagement is carried with the wave generator major elliptical axis. When this engagement zone is propagated 360° around the circumference of the circular spline, the flexspline which contains fewer teeth than the circular spline, will lag by that fewer number of teeth relative to the circular spline. Through this gradual and continuous engagement of slightly offset teeth, every rotation of the wave generator moves the flexspline a small angle back on the circular spline, and through this unconventional mechanism, gear ratios up to 320:1 can be achieved in a single transmission.

In numerous robotic control techniques such as feedback linearization, computed torque method and some adaptive control schemes, the actuator torque is taken to be the control input [6], [8], [9]. This can be only accomplished through torque feedback at each joint of the robot [12]. In order to apply torque feedback on the robot joint, it is necessary to measure the transmitted torque through the actuator transmission mechanism. Conventionally, torque sensor are placed in the output transmission line of the robot [5], [10]. However, for a harmonic drive transmission, which has an elastic element, the flexspline, there is no advantage to add an additional compliant element and thereby reduce the joint stiffness. In this paper we propose using the built-in torque sensor for harmonic drives [2], [17]. This method proved to be an economical and effective way of torque sensing for harmonic drives in our setup, as claimed by Hashimoto *et al.* [3]. In our testing station a Wheatstone bridge of four Rosette strain-gauges is utilized to sense the torsional torque transmitted through the flexspline. A practical and accurate method is proposed to mount the strain-gauges on the flexspline in order to minimize any radial or circumferential misplacement of each strain-gauge.

One important characteristic of harmonic drive torque transmission, is a high frequency oscillation in the output torque signal. These oscillations named torque ripples, whose principal frequency of oscillation (in radians per second) is twice the motor velocity (in radians per second), are mainly caused by harmonic drive gear meshing vibration. The dependence of the frequency content of the torque ripples on the velocity makes it possible to model them as a simple harmonic oscillator, and to employ a Kalman filter to predict and filter them from the torque measurement. If only low-frequency torque control is desired [14], the high-frequency ripples may be

H. D. Taghirad is with the Department of Electrical Engineering, K. N. Toosi University of Technology, Tehran, Iran, 16314 (e-mail: taghirad@eetd.kntu.ac.ir).

P. R. Bélanger is with the Center for Intelligent Machines, McGill University, Montréal, P.Q., H3A 2A7 Canada (e-mail: pbelanger@fgsr.mcgill.ca).

Publisher Item Identifier S 0018-9456(99)09538-8.

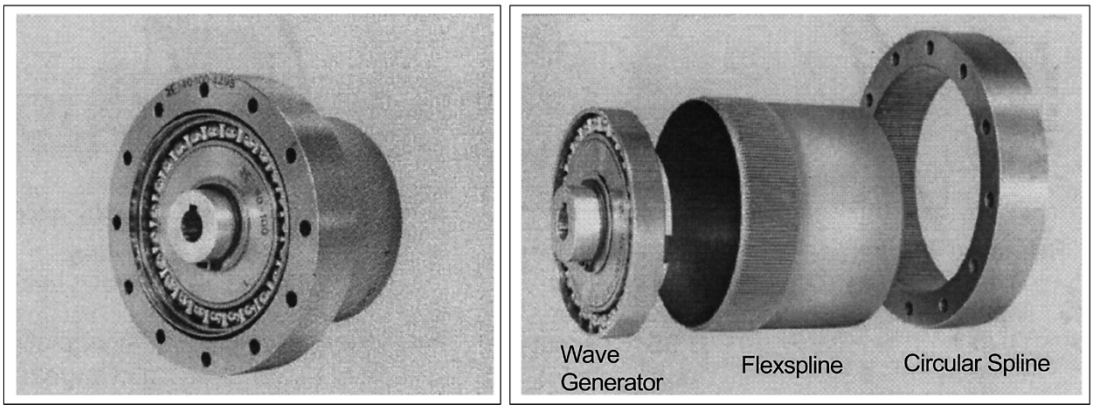

Fig. 1. Harmonic drive components.

removed by estimating them via Kalman filtering. This is more efficient than simple low-pass filtering, because it uses the known structure of the torque signal. The Kalman filter is also used to cancel any mechanical misalignment torque signature on the measured torque. Many torque sensors exhibit the limitation of being sensitive to the torques applied on the direction perpendicular to their axis of measurement. In our setup a similar torque signature was observed on the measured torque, whose source of generation is the misalignment of the harmonic drive shaft and the load. The frequency of misalignment torque (in radians per second), as it can be intuitively identified from its source of generation, is found to be exactly the same as the output shaft velocity (in radians per second). Therefore, by adding another block to the harmonic oscillator model we managed to estimate the misalignment component of the measured torque. The performance of the on-line implemented Kalman filter for torque ripple and misalignment torque cancellation is shown to be quite fast and accurate.

Finally, the combination of an accurate and practical method of torque sensing technique with the implementation of Kalman estimation technique, introduces an intelligent sensor for harmonic drive. This sensor can be economically added to many robot manipulators, in order to build a near-ideal torque source required for many robotic control strategies. The experimental results obtained using this intelligent torque sensor in a robust torque control implementation for our experimental setup [12], [13], proves that intelligent built-in torque sensors are viable and economical means to measure harmonic drive transmitted torque and to employ them for torque feedback strategies.

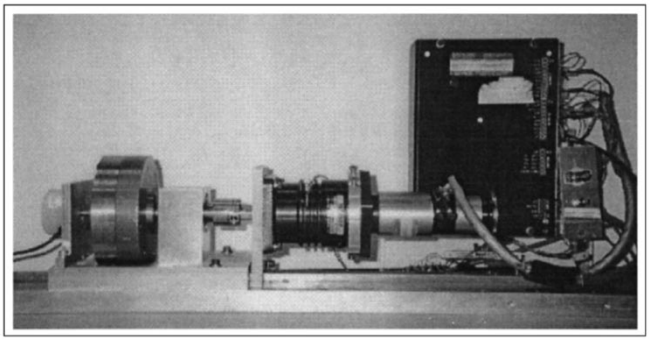

Fig. 2. A picture of the experimental setup.

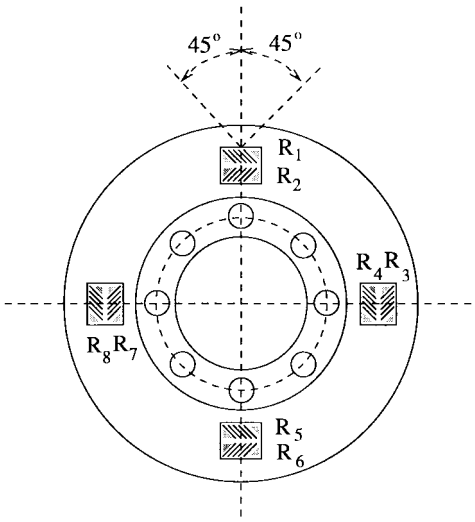

Fig. 3. Position of four Rosette strain-gauges on the flexspline diaphragm.

II. Experimental Setup

A harmonic drive testing station is employed to monitor the behavior of the system. A picture of the setup is illustrated in Fig. 2, in which the harmonic drive is driven by a dc motor, and a load inertia is used to simulate the robot arm. In this setup, a brushed dc motor from Electro-Craft is used. Its weight is 1360 grams, with maximum rated torque of 0.15 Nm, and torque constant of 0.0543 Nm/amp. The servo amplifier is a 40 W Electro-Craft power amplifier. The harmonic drive is from RHS series of HD systems, with gear ratio of 100:1, and rated torque of 40 Nm. The flexspline diameter is 46 mm, and its length is 49 mm.

The setup is equipped with a tachometer to measure the motor velocity, and an encoder on the load side to measure the output position. The current applied to the dc motor is measured from the servo amplifier output. The output torque is measured by a Wheatstone bridge of strain gauges mounted directly on the flexspline, whose output is conditioned and am-

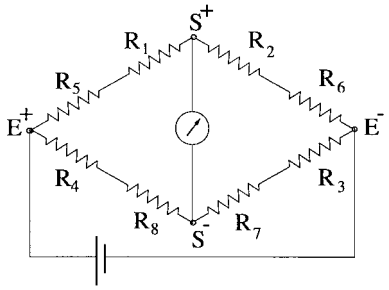

Fig. 4. Strain-gauges Wheatstone bridge network.

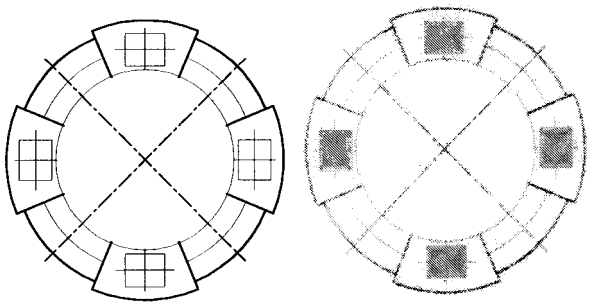

Fig. 5. Proposed transparent film for accurate strain-gauge placement.

plified. To amplify the output signal, a variable range amplifier with gain 1000 is used, while it generates 10 V dc as input voltage to the Wheatstone bridge. The details of built-in torque sensor will be elaborated in Section III. The measurement signals were processed by several data acquisition boards and monitored by a C-30 Challenger processor executing compiled computer C codes [11].

III. Built-In Torque Sensor

As illustrated in Fig. 3, four Rosette strain-gauges are mounted on the diaphragm part of the flexspline. A Rosette stain-gauge consist of two separate strain-gauges perpendicularly mounted on one pad. For a clockwise torque exerted on the flexspline illustrated in Fig. 3 strain-gauge R_1 is under compression while strain-gauge R_2 is under tension. Similarly all odd-indexed strain-gauges illustrated in Fig. 3 are under compression, while the others are under tension. Thus, a Wheatstone bridge of strain-gauges as illustrated in Fig. 4 can transduce the torsion into a difference voltage. The reason why Rosette strain-gauges are necessary for harmonic drive built in torque sensor, as explained in [3], is to compensate for the elliptical shape of the flexspline. If the strain caused by applied torque is named ϵ_t, while the strain caused by the elliptical shape of flexspline is called ϵ_w, Hashimoto *et al.* [4] illustrated that the strain applied to strain-gauge R_1, and R_2 are

$$\begin{cases} \epsilon_1 = \epsilon_t + \epsilon_w \\ \epsilon_2 = -\epsilon_t + \epsilon_{w'} \end{cases} \tag{1}$$

where $\epsilon_{w'}$ is assumed in [3] to be a sinusoidal modulation of ϵ_w. Thus,

$$\epsilon_1 - \epsilon_2 = 2\epsilon_t + \Psi_0 \sin(2\beta) \tag{2}$$

In order to cancel the modulation $\Psi_0 \sin(2\beta)$ and to detect the actual torsional strain ϵ_t the information from strain-gauges R_3, and R_4 is necessary. These strain-gauges are located at an angle of 90° from Strain-gauges R_1 and R_2, and therefore:

$$\epsilon_3 - \epsilon_4 = 2\epsilon_t + \Psi_0 \sin(2\beta - \pi) \tag{3}$$

Therefore, a Wheatstone bridge, constructed from strain-gauges R_1 to R_4 is sufficient to produce a difference voltage proportional to the torsional strain ϵ_t as following

$$\begin{aligned} E_{\text{out}} &= \frac{K}{4}(\epsilon_1 + \epsilon_3 - \epsilon_2 - \epsilon_4)E_{\text{sup}} \\ &= K\epsilon_t E_{\text{sup}} \end{aligned} \tag{4}$$

in which K is the gauge factor, and E_{out} and E_{sup} denote output and supply voltages, respectively.

Although, only two Rosette strain-gauges are sufficient to extract the torsional strain, two other Rosette strain-gauges are introduced to maintain symmetry, and to minimize the effect of positioning error. Sensing inaccuracies are caused by radial, circumferential, and angular positioning error. Radial positioning error occurs when the gauges are placed on different radii from the center of the flexspline. As shown in Fig. 3 even without any radial misplacement of the strain-gauges, radial error exists, since strain-gauges R_1 and R_2 are placed at different radii. However, by using four Rosette strain-gauge, as illustrated in Fig. 3, this error will be compensated by strain-gauges R_5, and R_6 which are located in the reverse position.

Circumferential positioning error occurs when two Rosette strain-gauges are mounted in an angle different than 90° from each other. This positioning error introduces more sensing inaccuracies than radial positioning error [4], [16]. Angular positioning error occurs when a Rosette strain-gauge is not mounted perpendicular to the flexspline's axis of rotation. This positioning error also introduces sensing inaccuracy similar to the circumferential positioning error. To minimize the positioning error, we propose a method using a specially-designed transparent film for the strain-gauges placement. As illustrated in Fig. 5, an accurate drawing of the strain-gauge placement positions is printed on a transparent film using a laser printer with the finest possible lines. Then the strain-gauges are placed on the transparent film using a microscope. By this means all positioning errors are reduced to a minimum, and as examined in our testing station to other placement methods, the sensing inaccuracy is minimized. When the strain-gauges are mounted on the transparent film as illustrated in Fig. 5, the transparent film is placed on the flexspline and the strain-gauges are cemented on the surface. The final configuration of the wired strain-gauges are illustrated in Fig. 6.

IV. Torque Sensor Calibration

To examine the dynamics of the torque sensor and to calibrate it, we locked the harmonic drive wave generator, and applied a known torque on the flexspline. The locking device is a simple shaft resembling the motor shaft, which can be fixed to the ground. The output torque is applied using arm and weight method. The torque calibration details of loading

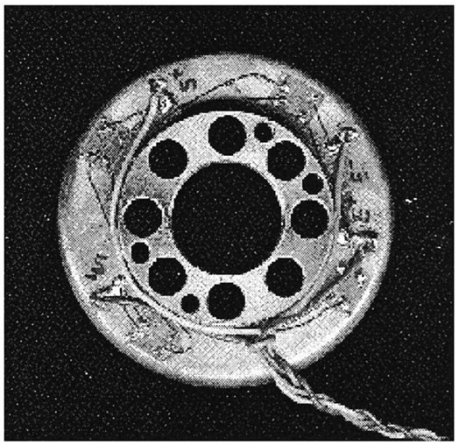

Fig. 6. Harmonic drive built-in torque sensor.

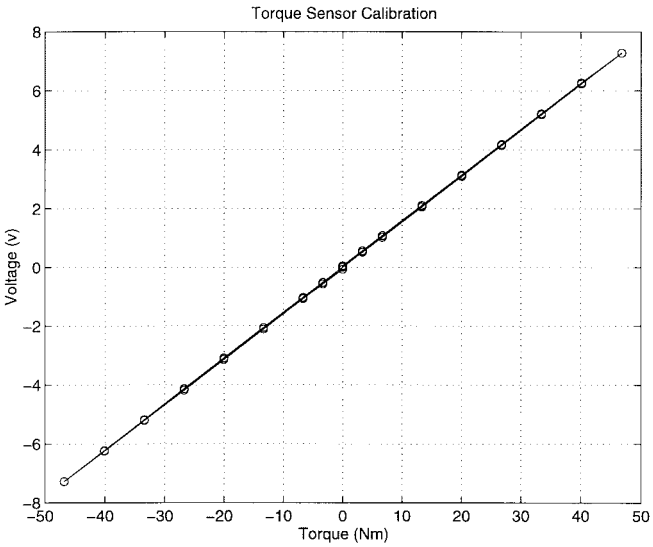

Fig. 7. Torque sensor calibration results for full-range loading.

TABLE I
TORQUE SENSOR CALIBRATION RESULTS

Torque Sensor Gain	Consistency Measure
6.60 Nm/V	2%

and unloading some weight on the arm, in both direction. This experiment is repeated at different flexspline positions, to check the position dependence of the torque sensor. Also low-range and full-range loading experiments are tested at each position to evaluate the nonlinearity of the torque sensor. A typical result for full-range loading experiment is shown in Fig. 7. These data are best fitted by a straight line using least-squares approximation. In least-square approximation, a model representation is assumed for the input-output relationship. In this representation the explicit relationship between the unknown quantities (in this case only the sensor gain) and the measurements are an affine function of the unknown quantity

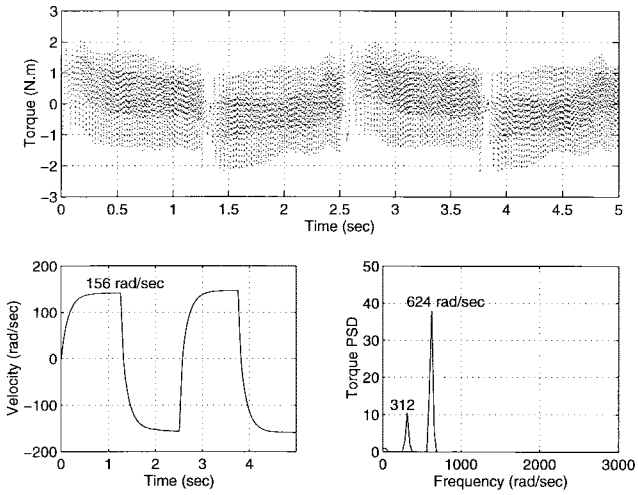

Fig. 8. Measured Torque and velocity and the power spectrum of the measured torque with peaks at multiples of the velocity.

(denoted $\boldsymbol{\theta}$) and can be expressed as:

$$\mathbf{A}\boldsymbol{\theta} = \mathbf{b} + \mathbf{n} \tag{5}$$

where in general $\mathbf{A}$ is an $m \times n$ matrix called the *observation matrix*, $\boldsymbol{\theta}$ is an $n \times 1$ column vector of identification parameters called *parameter vector*, $\mathbf{b}$ is an $m \times 1$ column vector called the *measurement vector*, and $\mathbf{n}$ is an $m \times 1$ vector called the *measurement noise*, where $\mathbf{n}$ is assumed to be zero-mean. If there is more measurements than unknowns, i.e. $m > n$, (5) constitutes overdetermined system of equations. The extra measurements are used to offset the effects of the noise. The objective of least-squares estimation is to find an estimate of the model parameter, called $\hat{\boldsymbol{\theta}}$, which approximately solves

$$\mathbf{A}\hat{\boldsymbol{\theta}} \approx \mathbf{b} \tag{6}$$

with minimum least-squares error. Equation (6) is called a *linear regression model* and $\hat{\boldsymbol{\theta}}$ is called the *least-squares solution*. If $\mathbf{A}$ is of full column rank, the least-squares solution can be expressed in terms of *Moore–Penrose generalized inverse* or *pseudo-inverse* of the rectangular matrix $\mathbf{A}$,

$$\hat{\boldsymbol{\theta}} = \mathbf{A}^{\dagger}\mathbf{b} \tag{7}$$

where

$$\mathbf{A}^{\dagger} := (\mathbf{A}^T\mathbf{A})^{-1}\mathbf{A}^T \tag{8}$$

The estimated torque sensor gain for each experiment is calculated from (7). However, this gain is deemed acceptable, only if it is consistent for other experiments. By consistency we mean a statistical measure, namely *the ratio of the standard deviation to the average value of estimated parameter for different experiments* [15]. If this measure is small, we have a good consistency for different experiments, and the final gain is obtained from the average value of the estimated gain for different experiments. The final gain is obtained by this method for eight experiments, and the result is given in Table I, where

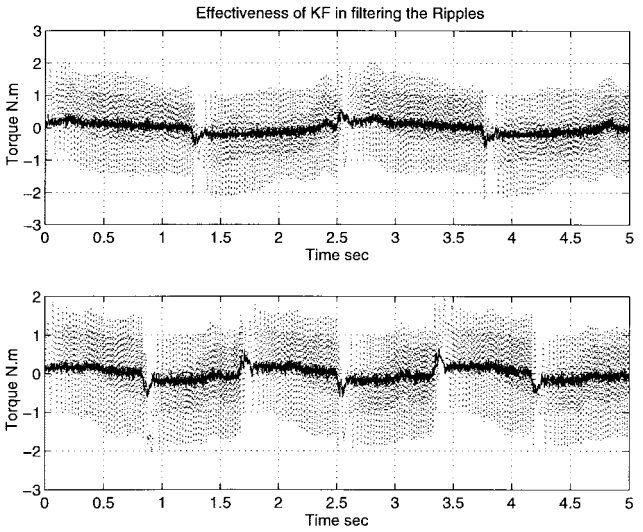

Fig. 9. Kalman filter performance to cancel torque ripples. Dotted: Measured torque, Solid: Kalman filtered torque.

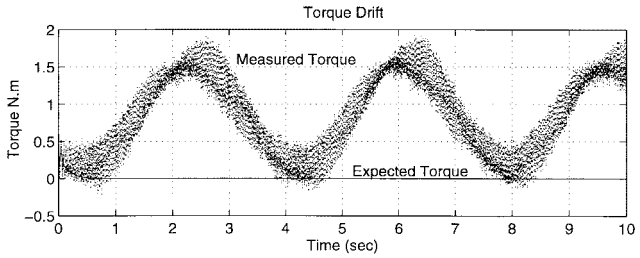

Fig. 10. Misalignment torque signature on the measured torque.

the gain is 6.6 Nm/V, with a low consistency measure of 2%. Note that to experiment the thermal stability of the system, the calibration tests are performed under different temperatures, ranging from 5° to 35°C. The change of operating temperature cause no significant effect on the calibration results. The low consistency measure in the result illustrates that the torque sensor is quite linear, it is not position dependent, and it is not sensitive to operating temperature. Moreover, the torque sensor gain is consistent for different operating conditions.

V. Torque Ripple Compensation

One important characteristic of harmonic drive torque transmission as observed in free motion experiments, is a high frequency oscillation in output torque signal (See torque curve in Fig. 8). These oscillation, named torque ripples, were also observed by other researchers [1]. Torque ripples are caused mainly by harmonic drive gear meshing vibration. Harmonic drive gear meshing vibration introduces a real torque oscillation which can be observed in the end effector motions of robots using harmonic drives and even sensed by hand when back-driving the harmonic drive. Its principal frequency of oscillation (in radians per second) is twice the motor velocity (in radians per second), for the gear teeth in harmonic drives are meshing in two zones. A small fraction of the torque ripples are caused by the nonideal torque

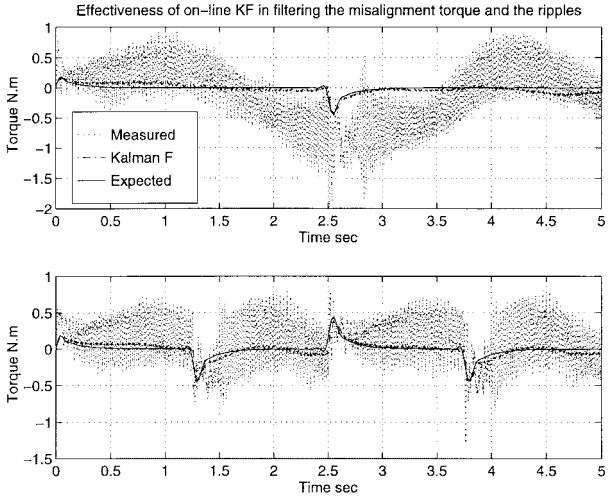

Fig. 11. Kalman filter performance to cancel torque ripples, and misalignment torque for two typical experiments.

measurement, because of the direct attachment of strain gauges on the flexspline.

Since the flexspline has an elliptical shape, strain gauges mounted on the flexspline are subjected to unwanted strain caused by the elliptical shape. Hashimoto [3], proposed using at least two pairs of Rosette strain gauges to compensate for this unwanted strain. However, ideal compensation is possible only if there is no positioning error of strain-gauges. As explained in Section III it has been shown however, that using four Rosette strain-gauges, and using an accurate method to mount the strain-gauges will reduce the amplitude of the torque ripple to a minimum. Unfortunately the frequency of torque ripples (in radians per second) introduced by the nonideal behavior of the sensor is also twice the motor speed (in radians per second), since the major axis of the ellipse is traveling twice as fast as the wave generator. This make it impossible to discern the true ripples caused by the gear meshing vibration from that caused by nonideal measurement. As illustrated in Fig. 8, the power spectrum of the measured torque plotted for the time interval 0.8 to 1.1 s when the velocity is almost flat and about 156 rad/s shows two peaks at 312, and 624 rad/s. This confirms the existence of the fundamental frequency of the oscillation as twice the velocity and shows the significance of the next important first-harmonic frequency of four times the velocity. The dependence of the frequency content of the torque ripples on the velocity makes it possible to model them as a simple harmonic oscillator, and to employ a Kalman filter to predict and filter them from the torque measurement. If only low-frequency torque control is desired [12], the high-frequency ripples may be removed by estimating them via Kalman filtering. This is more efficient than simple low-pass filtering, because it uses the known structure of the torque signal.

A fourth-order harmonic oscillator error model can characterize both the fundamental and first-harmonic frequency content of the torque ripple. This can be represented by the

following time-varying discrete state space form:

$$\begin{cases} \mathbf{x}(k+1) = \left[\begin{array}{c|c} \boldsymbol{\Phi}_1(k) & \mathbf{0} \\ \hline \mathbf{0} & \boldsymbol{\Phi}_2(k) \end{array}\right]\mathbf{x}(k) + \mathbf{w}(k) \\ y(k) = [1 \quad 0 \quad 1 \quad 0]\mathbf{x}(k) + v(k) \end{cases} \tag{9}$$

where

$$\boldsymbol{\Phi}_i(k) = \begin{bmatrix} \cos(\omega_i(k)T_s) & \sin(\omega_i(k)T_s) \\ -\sin(\omega_i(k)T_s) & \cos(\omega_i(k)T_s) \end{bmatrix} \tag{10}$$

in which T_s is the sampling period, and $\omega_1(k) = 2\dot{\theta}(k)$, $\omega_2(k) = 4\dot{\theta}(k)$, and $\dot{\theta}(k)$ is the motor shaft velocity in rad/s at time step k, hence $\boldsymbol{\Phi}_i(k)$ is a time-varying matrix adapting with changes in the velocity. Moreover, y is the torque ripple, which needs to be observed from the torque measurement by having a crude model for the expected torque. If measured torque is indicated by T_{meas}, and the expected torque is indicated by T_{exp} then torque ripple $y(k) = T_{\text{meas}}(k) - T_{\text{exp}}(k)$, while the difference between true torque and the crude estimate of the expected torque is encapsulated by the measurement errors in $v(k)$ in (9). Therefore, no accurate model for the expected torque T_{exp} is necessary and hence, for free motion experiments the expected torque can be estimated simply by the inertial part of the output torque which is the load inertia multiplied to the load acceleration. The first two elements of the state $\mathbf{x}$ consists of the component of the torque ripple due to the fundamental frequency ω_1, and its derivative, while the next two elements are those components of torque ripple due to the first-harmonic frequency ω_2, and its derivative. Therefore, the total torque ripple is calculated by adding the first and third element of the state. $\mathbf{w}(k)$ characterizes the other frequency components of the torque ripples which will not be estimated in this model.

Using the fourth-order harmonic oscillator model for the torque ripples, a prediction-type time-varying Kalman filter algorithm is applied to estimate the torque ripples [7]. A prediction-type estimate is computationally faster than a current-estimate type of Kalman filter, and therefore preferable for online implementation. Assuming that the process noise $\mathbf{w}(k)$ and measurement noise $v(k)$ are zero-mean Gaussian white and have covariances defined by $\mathbf{Q}$ and R as

$$E\{\mathbf{w}(k)\mathbf{w}^T(k)\} = \mathbf{Q}, \quad E\{v(k)v^T(k)\} = R \tag{11}$$

the states estimates is calculated using Kalman filter formulation [7] as

$$\hat{\mathbf{x}}(k+1) = \boldsymbol{\Phi}(k)\hat{\mathbf{x}}(k) + \mathbf{K}_e(k)[\mathbf{y}(k) - \mathbf{C}(k)\hat{\mathbf{x}}(k)] \tag{12}$$

in which the Kalman filter gain $\mathbf{K}_e(k)$ will be updated from

$$\mathbf{K}_e(k) = \boldsymbol{\Phi}(k)\mathbf{P}(k)\mathbf{C}^T(k)[R(k) + \mathbf{C}(k)\mathbf{P}(k)]\mathbf{C}^T(k)]^{-1} \tag{13}$$

$$\mathbf{P}(k+1) = \mathbf{Q}(k) + [\boldsymbol{\Phi}(k) - \mathbf{K}_e(k)\mathbf{C}(k)]\mathbf{P}(k)\boldsymbol{\Phi}^T(k). \tag{14}$$

Since the measurement signal $y(k)$ is a scalar, its covariance matrix $R(k)$ is also a scalar, and no matrix inversion is required for online implementation of the Kalman filter gain given in (13). Fig. 9 illustrates the performance of the Kalman filter implemented on line with a sampling frequency of 1 kHz to estimate and filter the torque ripples for two typical experiments, in which $\mathbf{Q} = 10^3\ \mathbf{I}_{4\times4}$ and $R = 1$. The performance of the Kalman filter for torque ripple cancellation is shown to be quite fast and accurate.

VI. Misalignment Torque Compensation

The Kalman filter can be used not only to estimate the torque ripples, but also to cancel any mechanical misalignment torque signature on the measured torque. Many torque sensors exhibit the limitation of being sensitive to the torques applied on the direction perpendicular to their axis of measurement. In our setup after repeated use of the harmonic drive system for different experiments, a similar torque signature was observed on the measured torque. Fig. 10 illustrates a simple experiment in which the harmonic drive is driven by a constant velocity but the measured torque exhibit a sinusoidal trend. The expected torque, the solid line in Fig. 10, is constant after a short time of acceleration, but the measured torque, dotted lines, displays a sinusoidal behavior. After examining the system accurately, the source of this torque signature is found to be the misalignment of the harmonic drive shaft and the load. By disassembling the system and carefully reassembling it, the peak to peak amplitude of this misalignment signature was reduced from 10 Nm to less than 2 Nm. However, in practice it is quite expensive, and probably infeasible to perfectly align all the moving components. Fortunately, the sinusoidal feature of this misalignment torque makes it possible to accurately estimate them with an error model.

The frequency of misalignment torque (in radians per second), as it can be intuitively identified from its source of generation, is exactly the same as the output shaft velocity (in radians per second). Therefore, adding another block to the harmonic oscillator model [given in (9)] of the system with frequency $\omega_3(k) = \text{vel}(k)/(\text{Gear Ratio})$, will estimate the misalignment component of the measured torque. Using this sixth order model for the torque ripple and misalignment torque together, Fig. 11 illustrates the Kalman filter performance in canceling those elements for two typical experiments. The Kalman filtered torque is shown to cancel the torque ripples and misalignment torque quite accurately. These results are obtained using an online Kalman filter implementation on the system with sampling frequency of 1 kHz. In contrary to low-pass filtering which is incapable of extracting the misalignment torque from the measurements, Kalman filter estimation proved to be fast and accurate to filter both torque ripples and misalignment torque. Moreover, it is a reliable method for different operating ranges, and therefore, preferable for torque feedback.

VII. Conclusion

In this paper the built-in torque sensor for harmonic drive systems as first proposed by Hashimoto is examined in detail. By this method strain-gauges are directly mounted on the flexspline, and therefore, no extra flexible element is introduced into the system. To have minimum sensing inaccuracy, four Rosette strain gauges are employed using an accurate method of positioning. An accurate drawing of the strain-

gauge placement positions is printed on a transparent film, and the strain-gauges are placed on the transparent film using a microscope. Then the transparent film is accurately placed on the flexspline, and the strain-gauges are cemented on the surface. It is shown that employing this method reduces the positioning error to a minimum. Calibration of the torque sensor shows that the sensor is performing linearly and the torque readings are not dependent to the position of the flexspline.

One important characteristic of harmonic drive torque transmission, as observed in free motion experiments, is a high frequency oscillation in the output torque signal. To cancel these oscillation named torque ripples from the measured torque, Kalman filter estimation is employed. Due to the dependence of the frequency content of the torque ripples on the wave generator velocity, a simple forth order harmonic oscillator proved to accurately model the torque ripples. The performance of Kalman filter to cancel the torque ripples from torque measurements is shown to be very fast and accurate. Moreover, the error model is extended to incorporate any misalignment torque signature. By on line implementation of the Kalman filter incorporating a sixth order model, it is shown that this method is a fast and accurate way to filter torque ripples and misalignment torque, and hence, this intelligent built-in torque sensor is preferable for torque feedback.

ACKNOWLEDGMENT

The authors would like to express their appreciation to A. Helmy for his involvement in the experiments. CAE and ISE contributed the equipment used in the setup.

REFERENCES

[1] I. Godler, K. Ohnishi, and T. Yamashita, "Repetitive control to reduce speed ripple caused by strain wave gearing," in *Proc. IECON*, 1994, vol. 2, pp. 1034–1038.
[2] M. Hashimoto, "Robot motion control based on joint torque sensing," in *Proc. IEEE Int. Conf. Robotics Automation*, 1989, pp. 256–261.
[3] M. Hashimoto, Y. Kiyosawa, H. Hirabayashi, and R. P. Paul, "A joint torque sensing technique for robots with harmonic drives," in *Proc. IEEE Int. Conf. Robotics Automation*, Apr. 1991, vol. 2, pp. 1034–1039.
[4] M. Hashimoto, Y. Kiyosawa, and R. P. Paul, "A torque sensing technique for robots with harmonic drives," *IEEE Trans. Robot. Automat.*, vol. 9, pp. 108–116, Feb. 1993.
[5] R. Hui, N. Kircanski, A. Goldenberg, C. Zhou, P. Kuzan, J. Weircienski, D. Gershon, and P. Sinha, "Design of the iris facility—A modular, reconfigurable and expandable robot test bed," in *Proc. IEEE Int. Conf. Robotics Automation*, 1993, vol. 1, pp. 155–160.
[6] S. Nicosia and P. Tomei, "On the feedback linearization of robots with elastic joints," in *Proc. IEEE Conf. Decision Control*, 1988, vol. 1, pp. 180–185.
[7] K. Ogata, *Discrete-Time Control Systems.* Englewood Cliffs, NJ: Prentice-Hall, 1995.
[8] M. W. Spong, "Adaptive control of flexible joint manipulators," *Syst. Contr. Lett.*, vol. 13, pp. 15–21, July 1989.
[9] M. W. Spong, J. Y. Hung, S. Bortoff, and F. Ghorbel, "Comparison of feedback linearization and singular perturbation techniques for the control of flexible joint robots," in *Proc. American Control Conf.*, 1989, vol. 1, pp. 25–30.
[10] D. Stokic and M. Vukobratovic, "Historical perspectives and state of the art in joint force sensory feedback control of manipulation robots," *Robotica*, vol. 11, pp. 149–157, Mar.–Apr. 1993.
[11] H. D. Taghirad, "Application of Kalman filter for intelligent built-in torque sensor of harmonic drives," Tech. Rep. TR-CIM-97-06, Center for Intelligent Machines, McGill Univ., Montreal, P.Q., Canada, Apr. 1997.
[12] H. D. Taghirad and P. R. Belanger, "Intelligent torque sensing and robust torque control of harmonic drive under free-motion," in *Proc. IEEE Int. Conf. Robotics Automation*, Apr. 1997, vol. 2, pp. 1749–1754.
[13] H. D. Taghirad and P. R. Belanger, "Robust torque control of harmonic drive under constrained motion," in *Proc. IEEE Int. Conf. Robotics Automation*, Apr. 1997, vol. 1, pp. 248–253.
[14] H. D. Taghirad and P. R. Belanger, "H-∞ based robust torque control of harmonic drive system under constrained- and free-motion applications," in *Proc. IEEE Int. Conf. Control Applications*, Sept. 1998, vol. 2, pp. 990–994.
[15] H. D. Taghirad and P. R. Belanger, "Modeling and parameter identification of harmonic drive systems," *J. Dyn. Syst., Meas., Contr.*, vol. 120, pp. 439–444, Dec. 1998.
[16] H. D. Taghirad, P. R. Belanger, and A. Helmy, "An experimental study on harmonic drive," Tech. Rep., Int, Submarine Eng, Ltd., Port Coquitlam, B.C., Canada, 1996.
[17] ———, "Intelligent built-in torque sensor for harmonic drive system," in *Proc. 1997 IEEE Instrumentation Measurement Technol. Conf.*, May 1997, vol. 1, pp. 969–974.

Hamid D. Taghirad received the B.Sc. degree in mechanical engineering from Sharif University of Technology, Tehran, Iran, in 1989, the M.Eng. in mechanical engineering in 1993, and the Ph.D. in electrical engineering in 1997, both from McGill University, Montréal, P.Q., Canada.

He is an Assistant Professor with the Electrical Engineering Department, and the head of Industrial Control Laboratory at K.N. Toosi University of Technology, Tehran. His research interest are robotic manipulator design and control, applied industrial control, and robust control.

P. R. Bélanger, photograph and biography not available at the time of publication.